The Thymidine Phosphorylase Imaging Agent ^{123}I-IIMU Predicts the Efficacy of Capecitabine

Nobuya Kobashi[1], Hiroki Matsumoto[1], Songji Zhao[2], Shunsuke Meike[1], Yuki Okumura[1], Tsutomu Abe[1], Hiromichi Akizawa[3], Kazue Ohkura[4], Ken-ichi Nishijima[2], Nagara Tamaki[2], and Yuji Kuge[2,5]

[1]Research Center, Nihon Medi-Physics Co., Ltd., Sodegaura, Japan; [2]Graduate School of Medicine, Hokkaido University, Sapporo, Japan; [3]Showa Pharmaceutical University, Machida, Japan; [4]Faculty of Pharmaceutical Sciences, Health Sciences University of Hokkaido, Ishikari-Tobetsu, Japan; and [5]Central Institute of Isotope Science, Hokkaido University, Sapporo, Japan

Recently, companion diagnostics with nuclear medicine techniques have been anticipated as more suitable means than biopsy for predicting treatment efficacy. The anticancer effect of capecitabine, an orally administered chemotherapeutic agent activated by thymidine phosphorylase (TP), is positively associated with tumor TP expression levels. This study aimed to assess whether TP imaging using a radiolabeled uracil derivative, ^{123}I-5-iodo-6-[(2-iminoimidazolidinyl)methyl]uracil (^{123}I-IIMU), could predict the efficacy of capecitabine treatment. **Methods:** Sensitivity to doxifluridine, a metabolite of capecitabine and direct substrate for TP, was assessed by water-soluble tetrazolium salt assays in vitro for 3 human colon cancer cell lines with different TP expression profiles. The intracellular uptake and retention of ^{123}I-IIMU were evaluated. Mice inoculated with each cell line were treated with capecitabine for 2 wk, and tumor growth was compared. In vivo distribution studies and SPECT/CT imaging of ^{123}I-IIMU were performed in inoculated mice. **Results:** In vitro experiments showed a positive relation between TP expression levels and doxifluridine sensitivity. In vitro studies revealed that intracellular uptake and retention of ^{123}I-IIMU were dependent on TP expression levels. In vivo experiments in inoculated mice showed that ^{123}I-IIMU accumulation in tumor tissue was in line with TP expression levels and susceptibility to capecitabine treatment. Moreover, SPECT/CT imaging of ^{123}I-IIMU in tumor-inoculated mice showed that ^{123}I-IIMU reflects TP expression levels in tumor tissues. **Conclusion:** ^{123}I-IIMU could be used as an in vivo companion diagnostic for predicting the efficacy of capecitabine treatment.

Key Words: companion diagnostics; doxifluridine; single photon emission computed tomography; uracil derivative

J Nucl Med 2016; 57:1276–1281
DOI: 10.2967/jnumed.115.165811

Molecularly targeted drugs such as gefitinib and trastuzumab have been widely used in cancer treatment. To select patients expected to respond to these medicines, in vitro companion diagnostics have been used in clinical practice to assess gene mutations or protein expression before administration. Companion diagnostics also decrease unnecessary adverse drug reactions while enabling patient stratification and facilitating drug development. Currently, biopsy samples or surgical specimens are used for in vitro companion diagnostics in clinical practice. However, several studies have evaluated companion diagnostics with imaging modalities (*1–3*). The folate receptor imaging agent ^{99m}Tc-etarfolatide was developed as a companion radiopharmaceutical agent for vintafolide, a conjugate of folic acid and a vinca alkaloid, for targeting folate receptors in cancer cells (*1–3*). ^{99m}Tc-etarfolatide had a higher sensitivity and specificity for the noninvasive detection of vintafolide-susceptible metastatic cancer foci than folate receptor immunohistochemistry using biopsy samples, suggested to result from changes in folate receptor expression over time or the heterogeneity of folate receptor expression among cancer lesions. Therefore, to avoid repeated biopsies and correctly evaluate the expression of target proteins difficult to examine with limited samples (e.g., the folate receptor), radiopharmaceutical companion diagnostics are more suitable than in vitro companion diagnostics. Additionally, other imaging agents such as ^{18}F-FAC for gemcitabine (*4*) and ^{18}F-misonidazole for tirapazamine (*5*) have been reported to predict the effect of anticancer drugs.

Capecitabine, an orally bioavailable drug and the prodrug of 5-fluorouracil, is a broadly used anticancer drug for colorectal, breast, and stomach cancer. It produces serious adverse reactions including hand–foot syndrome, diarrhea, and bone marrow suppression (*6,7*), and tumor response rates vary from 20% to 50% (*8–10*). Thymidine phosphorylase (TP), which is overexpressed in various tumors, catalyzes the reversible conversion of thymidine to thymine and 2-deoxy-D-ribose-1-phosphate (*11*). Capecitabine is absorbed through the intestine and metabolized to doxifluridine by carboxylesterases and cytidine deaminases in the liver. Doxifluridine is metabolized to active forms by TP in the liver and tumor tissues (Supplemental Fig. 1; supplemental materials are available at http://jnm.snmjournals.org) (*12*). Capecitabine-based chemotherapies have been reported to be more effective in tumors expressing high TP levels (*13–16*). However, in these studies, tumor TP expression levels were determined immunohistochemically in surgical specimens or biopsy samples. TP expression is heterogeneous even in primary tumors (*17*), differs between tumor and stromal cells and between the primary lesion and metastatic foci (*18*), and is affected by chemotherapy (e.g., taxanes, cyclophosphamide, anthracycline, and platinum) and radiotherapy (*19–23*). On the basis of these previous reports, TP imaging should be more suitable for predicting capecitabine efficacy than biopsy, similar to ^{99m}Tc-etarfolatide for vintafolide-susceptible tumors. Furthermore, if TP imaging could predict capecitabine response, nonresponder patients could be identified earlier without unnecessary adverse effects and have an opportunity to receive alternative medications.

Received Aug. 24, 2015; revision accepted Mar. 11, 2016.
For correspondence or reprints contact: Hiroki Matsumoto, Research Center, Nihon Medi-Physics Co., Ltd., 3-1 Kitasode, 299-0266 Sodegaura, Japan.
E-mail: hiroki_matsumoto@nmp.co.jp
Published online Apr. 7, 2016.
COPYRIGHT © 2016 by the Society of Nuclear Medicine and Molecular Imaging, Inc.

We previously designed, synthesized, and evaluated the radiolabeled TP inhibitor ^{125}I-5-iodo-6-[(2-iminoimidazolidinyl)methyl] uracil (^{125}I-IIMU) (Fig. 1) as a noninvasive TP imaging probe (*24*). ^{125}I-IIMU accumulated in cancer cells and tumor tissues depending on TP expression levels (*25–27*), suggesting that radiolabeled IIMU enables TP-specific image acquisition. Because TP is responsible for capecitabine activation, we hypothesized that ^{123}I-IIMU, as an imaging probe for SPECT, could be used to predict capecitabine efficacy in cancer patients. To test this hypothesis, we examined relations among TP expression levels, capecitabine sensitivity, and ^{123}I-IIMU accumulation in human colorectal cancer cell lines.

MATERIALS AND METHODS

Cell Cultures

The human colorectal cancer cell lines HCT116, WiDr, and DLD-1 were obtained from American Type Culture Collection and cultured in McCoy 5A, modified Eagle medium, and RPMI1640 culture medium, respectively, containing 10% fetal bovine serum and penicillin/streptomycin/neomycin at 37°C in 5% CO_2. All cell culture regents were purchased from Life Technologies Corp.

Cell Viability Assay

Cells were seeded at a density of 2×10^3 (HCT116), 8×10^3 (WiDr), and 3×10^3 (DLD-1) cells/well in 96-well plates and treated with doxifluridine (Santa Cruz Biotechnology), a metabolite of capecitabine, at concentrations of 391 nM to 200 μM for 48 h at 37°C. After incubation, viable cells were assessed using Cell Counting Kit-8 (Water-soluble Tetrazolium salts-8 colorimetric method; Dojindo Laboratories) according to the manufacturer's protocol. Absorbance at 450 nm was measured using a VersaMax microplate reader (Molecular Devices). Cell viability was expressed as the absorbance relative to the absorbance of untreated controls in each experiment and calculated as a percentage. The survival curves for each doxifluridine-treated cell line were constructed using GraphPad Prism (version 5.0; GraphPad Software), and the half maximal inhibitory concentration (IC_{50}) value of doxifluridine was calculated accordingly.

Transient Transfection with Small-Interference RNA (siRNA)

TP siRNA was synthesized by Japan Bio Services. The siRNA sequences were 5′-AUAGACUCCAGCUUAUCCAAGGUGC-3′ (sense) and 5′-GCACCUUGGAUAAGCUGGAGUCUAU-3′ (antisense) (*28*). Silencer Negative Control siRNA was purchased from Life Technologies Corp. HCT116 cells were transfected with 20 nM siRNA using Lipofectamine RNAiMAX (Life Technologies Corp.). After 72-h incubation, cells were collected for cell viability assay and Western blot.

Intracellular Uptake and Retention Studies

HCT116 and DLD-1 cells were seeded at a density of 5×10^5 cells/well in 6-well plates, washed twice with 0.01 M phosphate-buffered saline (0.0027 M KCl, 0.137 M NaCl), and placed in serum-free medium containing ^{123}I-IIMU (1 mL). For the cellular uptake assay, cells were incubated for 0.5, 1, and 2 h at 37°C. For the cellular efflux assay, cells were incubated with ^{123}I-IIMU for 2 h and then washed twice with ice-cold phosphate-buffered saline. After the tracer solution was removed, serum-free medium (1 mL) was added, and the cells were further incubated for 0.5, 1, and 2 h. After incubation for uptake or efflux, the cells were washed twice with ice-cold phosphate-buffered saline and lysed in 0.5 M NaOH (0.5 mL). Radioactivity in each aliquot was measured using a γ-counter (ARC-7001; Hitachi Aloka Medical) and normalized against the total protein concentration.

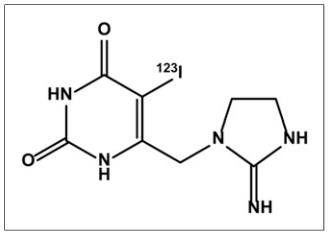

FIGURE 1. Structure of ^{123}I-IIMU.

Animal Model

Female BALB/c-*nu/nu* mice (5–8-wk-old) were purchased from CLEA. All animal studies were approved by the Laboratory Animal Care and Use Committee of Hokkaido University or Nihon Medi-Physics Research Center and conducted in accordance with the institutional guidelines of each institution. Tumor cells (2.0×10^6 cells) were suspended in serum-free culture medium, mixed with an equal volume of Matrigel (Becton, Dickinson and Co.), and subcutaneously inoculated in the right flank of mice. For SPECT/CT imaging, HCT116 and DLD-1 cells were inoculated in the right and left flank of mice, respectively. Experiments started when the average tumor volume was 250–400 mm^3.

Capecitabine Treatment

Capecitabine (Santa Cruz Biotechnology) was suspended in distilled water and orally administered (539 mg/kg/d) to tumor-inoculated mice for 5 d per week, as previously reported (*29*). Control tumor-inoculated mice were left untreated. To evaluate capecitabine antitumor effect, tumor size and body weight were measured twice per week. Tumor volume was calculated using a caliper according to the following equation: volume = height × width × depth × (π/6). Relative tumor size was calculated by dividing the tumor volume on any given day by that on the first day of treatment.

Biodistribution Studies

These studies were performed 15 d after inoculation. Under isoflurane/air anesthesia, saline containing ^{123}I-IIMU (667 kBq/0.1 mL) was injected through the tail vein. At 30 min after injection, tumor and control tissues were collected and weighed, and their radioactivity was measured using a single-channel γ-counter (Ohyo Koken Kogyo). Radioactivity was expressed as a percentage injected dose per gram of tissue.

SPECT/CT

SPECT/CT imaging was performed using an Inveon SPECT/CT scanner (Siemens Medical Solutions) with a double-head detector. Each head contained a 68×68 pixelated scintillator array. Each pinhole collimator had an aperture of 2.0 mm. The radius of rotation was 35 mm. Studies were performed 12 d after inoculation. A saline solution of ^{123}I-IIMU (25 MBq/0.1 mL) was injected through the tail vein under isoflurane anesthesia. At 45 min after administration, data were acquired for 30 min.

Immunohistochemistry

After SPECT/CT scanning, the mice were euthanized by exsanguination under deep isoflurane anesthesia, and tumor tissues were excised. Tumor tissues were fixed in 15% formalin for 48 h, paraffin-embedded, and sectioned at 4 μm. The sections were mounted on slides, deparaffinized, and rehydrated. Antigen retrieval was performed by heating the slides at 95°C in pH 9.0 ethylenediaminetetraacetic acid solution for 20 min. Endogenous peroxidase activity was blocked by treatment with 0.3% H_2O_2 for 10 min. The slides were incubated with Mousestain kit blocking reagent A (Nichirei Biosciences) and then with a mouse monoclonal anti-TP antibody (GF40-100UGCN; Merck) overnight at 4°C. Sections were then incubated with Mousestain kit blocking reagent B (Nichirei Biosciences), followed by incubation with Mousestain kit simple stain mouse MAX-PO (M) at room temperature. The sections were developed using diaminobenzidine (Dako) and counterstained with hematoxylin. Additionally, some sections were stained with hematoxylin and eosin using a standard protocol.

Statistical Analysis

Data are presented as the mean ± SEM. One-way or 2-way ANOVA and Tukey multiple-comparison tests were used to analyze capecitabine efficacy in vivo and in biodistribution experiments. A Student *t* test was used for other experiments. A *P* value of less than 0.05 was considered statistically significant.

RESULTS

Antiproliferative Activity of Doxifluridine in Cancer Cell Lines

Because capecitabine is converted to doxifluridine in the liver and then to 5-fluorouracil by TP in tumor cells (Supplemental Fig. 1), we used doxifluridine in our in vitro assay. TP expression levels in HCT116 cells were higher than those in WiDr or DLD-1 cells (Fig. 2A). HCT116 cells were more sensitive to doxifluridine treatment than WiDr and DLD-1 cells (Fig. 2B). The doxifluridine IC_{50} values for HCT116, WiDr, and DLD-1 cells were 26.4, 74.3, and 77.9 μM, respectively, suggesting that TP expression levels parallel the antiproliferative activity of doxifluridine in vitro. There was no statistically significant difference among IC_{50} values for the 3 cell types. TP siRNA transfection dramatically downregulated TP expression in HCT116 cells (Fig. 2C). After 50-μM doxifluridine treatment for 48 h, the viability of TP siRNA-transfected cells and negative control cells was 70.3% and 40.5%, respectively ($P < 0.01$) (Fig. 2D). Thus, downregulation of TP significantly inhibited doxifluridine anticancer activity.

Effect of Capecitabine in Transplanted Tumors

Capecitabine in vivo antiproliferative activity was evaluated in mice inoculated with HCT116, WiDr, or DLD-1 cells. Capecitabine inhibited the growth of tumors formed from HCT116 cells, whereas no significant change was observed in relative tumor size in mice inoculated with WiDr and DLD-1 cells compared with control (Fig. 3).

Intracellular ^{123}I-IIMU Uptake and Retention

To assess whether ^{123}I-IIMU could reflect TP expression differences among these cell lines, we performed intracellular uptake and retention studies. In HCT116 cells, ^{123}I-IIMU intracellular uptake increased with incubation time and was significantly higher than that in DLD-1 cells (Fig. 4A). In the efflux assay, 30.7% of the radioactivity before removing the tracer solution was retained by HCT116 cells at 2 h after removal, whereas only 1.23% was retained by DLD-1 cells (Fig. 4B).

^{123}I-IIMU Uptake by Transplanted Tumors

We further examined the biodistribution of ^{123}I-IIMU in mice carrying xenografts of the 3 cell lines. Radioactivity in HCT116, WiDr, and DLD-1 tumors at 30 min after injection was 0.99, 0.38, and 0.22 percentage injected dose per gram, respectively (Fig. 5A). Radiotracer levels in other tissues were similar across groups (Supplemental Table 1). Additionally, radioactivity levels in the thyroid gland and stomach, an indicator of in vivo deiodization, were low in these mice, as previously reported (*24*). These data indicate a positive relation between ^{123}I-IIMU accumulation and tumor expression levels of TP. Figure 5B shows that capecitabine antiproliferative activity in tumor-bearing mice is consistent with ^{123}I-IIMU accumulation in tissues from each tumor cell line.

SPECT/CT Imaging of ^{123}I-IIMU and Immunohistochemical Detection of TP

To assess whether ^{123}I-IIMU could detect high TP expression in tumors in vivo, we performed a SPECT/CT study (Fig. 6A).

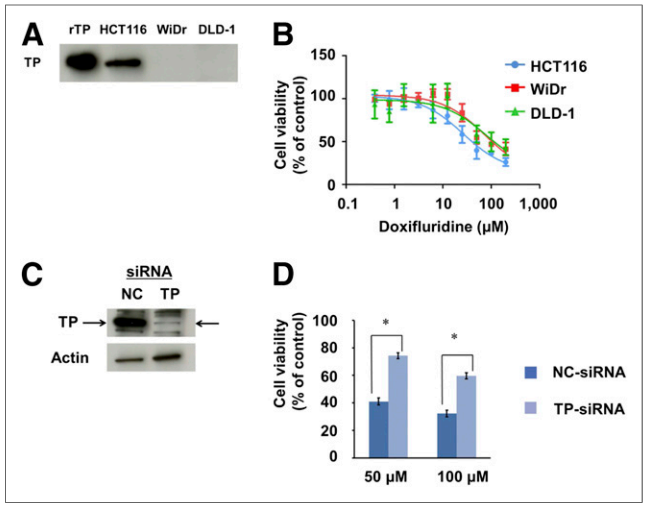

FIGURE 2. Effect of TP on doxifluridine antiproliferative activity in vitro. (A) Western blot analysis of TP expression in 3 colorectal cell lines, with recombinant TP protein (rTP) used as positive control. (B) Doxifluridine antiproliferative effect in colorectal tumor cells. Data are expressed as percentage absorbance relative to the control in each experiment ($n = 3$). (C) Western blot analysis of TP expression levels in negative control (NC) and TP siRNA-transfected HCT116 cells. Arrows show TP bands. (D) Antiproliferative effect of doxifluridine in siRNA-transfected HCT116 cells. Statistical analysis was performed using unpaired Student *t* test (*$P < 0.01$) ($n = 4$).

^{123}I-IIMU accumulated in xenografts of capecitabine-sensitive HCT116 cells but not in DLD-1–inoculated xenografts. In HCT116 tumors, ^{123}I-IIMU showed a high tumor-to-muscle ratio (Supplemental Table 1) and clearly enabled the detection of high TP expression in SPECT images. However, a large amount of ^{123}I-IIMU was distributed in the liver and small intestine (Supplemental Fig. 2). To confirm the TP expression levels in HCT116 and DLD-1 cells, HCT116 and DLD-1 tumors were excised after SPECT/CT imaging, sectioned, and immunohistochemically stained (Fig. 6B). High TP expression levels were observed in HCT116 tumors. Little TP expression was observed in DLD-1 tumors.

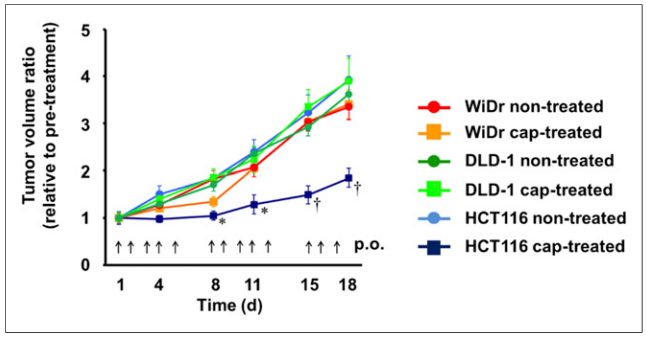

FIGURE 3. Effect of TP on tumor growth inhibition by capecitabine in mice inoculated with colorectal tumor cells. Tumor-inoculated mice were randomized for administration of 539 mg/kg/d of capecitabine (cap-treated) or no treatment (nontreated). Arrows indicate capecitabine administration. Statistical analysis was performed using 2-way ANOVA followed by Tukey multiple-comparison test (*$P < 0.05$, †$P < 0.01$ vs. HCT116 nontreated). Results are expressed as mean ± SEM ($n = 7$–10). p.o. = oral administration.

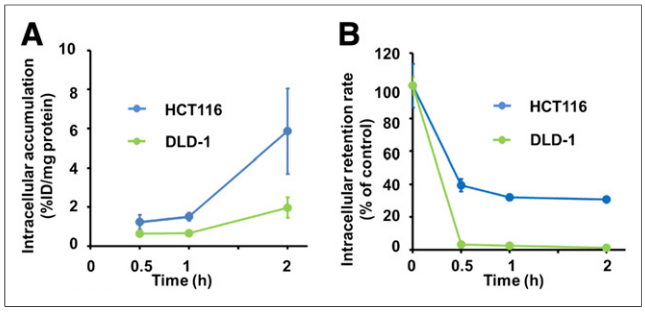

FIGURE 4. Dependence of ^{123}I-IIMU intracellular uptake and retention on TP expression levels in colorectal carcinoma cell lines. Intracellular uptake (A) and retention (B) of ^{123}I-IIMU in HCT116 and DLD-1 cells were dependent on TP expression levels. Results are expressed as mean ± SEM of triplicate experiments in 1 d. %ID/mg = percentage injected dose per milligram.

DISCUSSION

Antiproliferative activity of doxifluridine in vitro was higher in HCT116 cells, which have higher TP expression levels, than in WiDr and DLD-1 cells (Figs. 2A and 2B). TP downregulation significantly decreased sensitivity to doxifluridine (Figs. 2C and 2D). A previous study showed that the antiproliferative activity of doxifluridine in vitro was higher in HCT116 cells than in DLD-1 cells (*30*). Our results are consistent with this finding. We further investigated the relationship between the efficacy of capecitabine and TP expression levels in vivo (Fig. 3). The efficacy of capecitabine has been found to correlate with TP messenger RNA levels and TP activity in previous studies (*31,32*). These studies showed that HCT116 cells were susceptible to capecitabine treatment but neither WiDr nor DLD-1 cells were. Additionally, HCT116 had the highest TP activity among the 3 cell types, and DLD-1 had the lowest. Our results also correspond to these findings in vivo.

In vitro, intracellular uptake and retention of ^{123}I-IIMU were higher in HCT116 cells than in DLD-1 cells, with low TP expression (Figs. 4A and 4B). In our previous studies, we found high accumulation of ^{125}I-IIMU in high-TP-expressing A431 human epithelial carcinoma cells (*25,26*), and ^{125}I-IIMU accumulation was inhibited by adding unlabeled IIMU. These results showed that the uptake of radiotracer in tumor cells corresponded to TP expression levels. Additionally, in vivo biodistribution experiments showed higher uptake of ^{123}I-IIMU in HCT116 tumors than in the other tumors (Fig. 5A), and the antiproliferative effect of capecitabine against tumor growth in mice was associated with the accumulation of ^{123}I-IIMU in each cell line (Fig. 5B). In our previous studies, we investigated the biodistribution of ^{125}I-IIMU and ^{123}I-IIMU in mice (*25,27*). The radiolabeled tracers mainly accumulated in the liver and small intestine, consistent with our present results. Furthermore, we confirmed messenger RNA and protein levels of TP in various mouse tissues (*27*). We observed high TP expression in the liver and intestine, which corresponded to the observed high accumulation of radiolabeled IIMU (Supplemental Table 1). Taken together, our results show an association between ^{123}I-IIMU accumulation in tumor cells and capecitabine efficacy both in vitro and in vivo with the same cancer cell lines. However, it was not clear whether ^{123}I-IIMU SPECT/CT can detect differences between high- and low-TP-expressing tumor. Therefore, we performed a SPECT/CT study, in which ^{123}I-IIMU clearly detected HCT116 tumors with high TP expression levels (Figs. 6A and 6B), whereas the accumulation of ^{123}I-IIMU in DLD-1 tumors was negligible, indicating that ^{123}I-IIMU can discriminate tumor TP expression levels noninvasively. However, liver and small intestine metastasis may be difficult to visualize because we observed high physiologic accumulations of ^{123}I-IIMU in the liver and small intestine (Supplemental Fig. 2). This result was consistent with the biodistribution study (Supplemental Table 1).

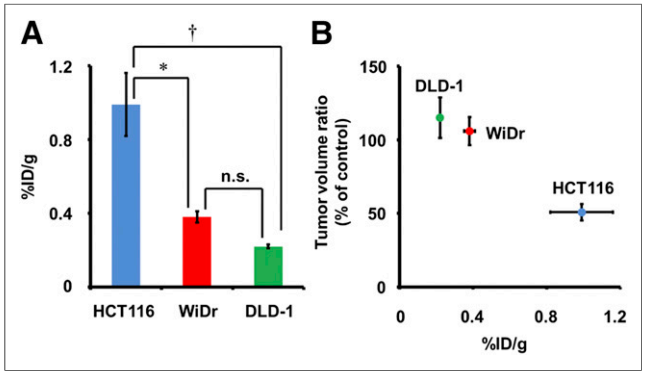

FIGURE 5. Relation between ^{123}I-IIMU accumulation in tumors and capecitabine effect on tumor growth using mice inoculated with tumor cell lines. (A) Accumulation of ^{123}I-IIMU in tumor-inoculated mice at 30 min after injection. Statistical analysis was conducted using 1-way ANOVA followed by Tukey multiple-comparison test (*$P < 0.05$, †$P < 0.01$, n.s. = not significant). (B) ^{123}I-IIMU accumulation in tumors was positively associated with effect of capecitabine on tumor growth at 18 d after pretreatment. Results are expressed as mean ± SEM of 3–10 independent experiments. %ID/g = percentage injected dose per gram.

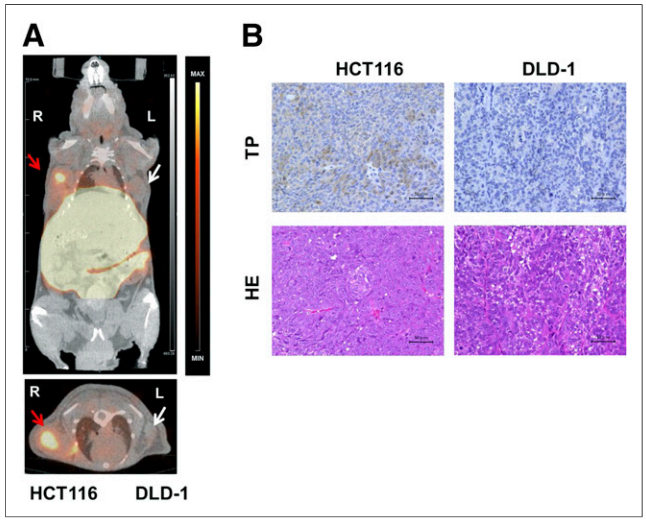

FIGURE 6. ^{123}I-IIMU imaging of mice inoculated with tumor cells and immunohistochemistry for TP at 45 min after injection. (A) ^{123}I-IIMU accumulation in tumor tissue depended on TP levels. Coronal (top) and transverse (bottom) images of ^{123}I-IIMU SPECT/CT. Red arrows indicate HCT116 tumor. White arrows indicate DLD-1 tumor. (B) Immunohistochemistry for TP (upper row) and hematoxylin and eosin (HE) staining (lower row) in HCT116 (left column) and DLD-1 (right column) tumor tissue sections from mouse that underwent SPECT/CT. The same experiments were conducted in different animals at 30 or 180 min after administration, yielding similar results (Supplemental Figs. 2 and 3). Scale bars = 50 μM. max = maximum; min = minimum.

^{99m}Tc-etarfolatide images as a biomarker to predict the antiproliferative activity of vintafolide did not always reflect immunohistochemical results because most surgical specimens for pathologic diagnosis had been obtained months or years earlier. Moreover, folate receptor expression levels in metastatic lesions differed from those in the primary tumor. However, in practice, technical and ethical issues prevent a pathologic diagnosis being performed in all surgical specimens and metastases to predict drug response. Additionally, similar studies have reported that TP expression levels in tumors affect capecitabine efficacy (*13–16*). Our results show that ^{123}I-IIMU has potential as a prognostic imaging biomarker for capecitabine efficacy. Because radiation and chemotherapy alter TP expression, whole-body TP measurement in real time using ^{123}I-IIMU would enable the more accurate prediction of treatment outcomes.

A limitation of our study is that we used only human colorectal cell lines. To further assess the potential use of ^{123}I-IIMU imaging, further experiments with cell lines derived from cancer in other organs such as breast, head, and neck are needed. Additionally, PET imaging with ^{124}I-IIMU could provide more informative images concerning quantification of TP. However, ^{124}I has a longer half-life and numerous higher-energy γ-emissions. With regard to commercial availability, ^{123}I is extensively used. Therefore, ^{123}I-IIMU would be more acceptable for initial clinical study. TP activates not only capecitabine but also 5-fluorouracil, doxifluridine, and S-1 (*33–37*). Therefore, ^{123}I-IIMU could likely predict the effect of treatment using all of these drugs. In vivo companion diagnostics using ^{123}I-IIMU and SPECT may provide optimized treatments and better quality of life for individual cancer patients.

CONCLUSION

We showed an association between TP expression levels determined noninvasively using ^{123}I-IIMU in tumor cells and the efficacy of capecitabine in vitro and in vivo, suggesting that ^{123}I-IIMU is a predictive imaging biomarker for the outcome of capecitabine treatment.

DISCLOSURE

The costs of publication of this article were defrayed in part by the payment of page charges. Therefore, and solely to indicate this fact, this article is hereby marked "advertisement" in accordance with 18 USC section 1734. This work was supported by the Creation of Innovation Centers for Advanced Interdisciplinary Research Areas Program of the Ministry of Education, Culture, Sports, Science, and Technology of Japan. Nobuya Kobashi, Shunsuke Meike, Yuki Okumura, Tsutomu Abe, and Hiroki Matsumoto are employees of Nihon Medi-Physics Co., Ltd. Hiromichi Akizawa, Kazue Ohkura, Ken-ichi Nishijima, Songji Zhao, Yuji Kuge, Hokkaido University, and Health Sciences University of Hokkaido have patent rights for ^{123}I-IIMU. No other potential conflict of interest relevant to this article was reported.

ACKNOWLEDGMENT

We thank Miho Ikenaga for performing the cell viability assay.

REFERENCES

1. Fisher RE, Siegel BA, Edell SL, et al. Exploratory study of ^{99m}Tc-EC20 imaging for identifying patients with folate receptor-positive solid tumors. *J Nucl Med.* 2008;49:899–906.
2. Morris RT, Joyrich RN, Naumann RW, et al. Phase II study of treatment of advanced ovarian cancer with folate-receptor-targeted therapeutic (vintafolide) and companion SPECT-based imaging agent (^{99m}Tc-etarfolatide). *Ann Oncol.* 2014;25:852–858.
3. Maurer AH, Elsinga P, Fanti S, et al. Imaging the folate receptor on cancer cells with ^{99m}Tc-etarfolatide: properties, clinical use, and future potential of folate receptor imaging. *J Nucl Med.* 2014;55:701–704.
4. Laing RE, Walter MA, Campbell DO, et al. Noninvasive prediction of tumor responses to gemcitabine using positron emission tomography. *Proc Natl Acad Sci USA.* 2009;106:2847–2852.
5. Rischin D, Hicks RJ, Fisher R, et al. Prognostic significance of ^{18}F-misonidazole positron emission tomography-detected tumor hypoxia in patients with advanced head and neck cancer randomly assigned to chemoradiation with or without tirapazamine: a substudy of trans-tasman radiation oncology group study 98.02. *J Clin Oncol.* 2006;24:2098–2104.
6. Bang YJ, Van Cutsem E, Feyereislova A, et al. Trastuzumab in combination with chemotherapy versus chemotherapy alone for treatment of HER2-positive advanced gastric or gastro-oesophageal junction cancer (ToGA): a phase 3, open-label, randomised controlled trial. *Lancet.* 2010;376:687–697.
7. Kang YK, Kang WK, Shin DB, et al. Capecitabine/cisplatin versus 5-fluorouracil/cisplatin as first-line therapy in patients with advanced gastric cancer: a randomised phase III noninferiority trial. *Ann Oncol.* 2009;20:666–673.
8. Saeki T, Kimura T, Toi M, Taguchi T. A pilot phase II study of capecitabine in advanced or recurrent breast cancer. *Breast Cancer.* 2006;13:49–57.
9. Blum JL, Jones SE, Buzdar AU, et al. Multicenter phase II study of capecitabine in paclitaxel-refractory metastatic breast cancer. *J Clin Oncol.* 1999;17:485–493.
10. Van Cutsem E, Findlay M, Osterwalder B, et al. Capecitabine, an oral fluoropyrimidine carbamate with substantial activity in advanced colorectal cancer: results of a randomized phase II study. *J Clin Oncol.* 2000;18:1337–1345.
11. Takebayashi Y, Yamada K, Miyadera K, et al. The activity and expression of thymidine phosphorylase in human solid tumours. *Eur J Cancer.* 1996;32A:1227–1232.
12. Bonotto M, Bozza C, Di Loreto C, et al. Making capecitabine targeted therapy for breast cancer: which is the role of thymidine phosphorylase? *Clin Breast Cancer.* 2013;13:167–172.
13. Schüller J, Cassidy J, Dumont E, et al. Preferential activation of capecitabine in tumor following oral administration to colorectal cancer patients. *Cancer Chemother Pharmacol.* 2000;45:291–297.
14. Lee SJ, Choi YL, Park YH, et al. Thymidylate synthase and thymidine phosphorylase as predictive markers of capecitabine monotherapy in patients with anthracycline- and taxane-pretreated metastatic breast cancer. *Cancer Chemother Pharmacol.* 2011;68:743–751.
15. Koizumi W, Okayasu I, Hyodo I, et al. Prediction of the effect of capecitabine in gastric cancer by immunohistochemical staining of thymidine phosphorylase and dihydropyrimidine dehydrogenase. *Anticancer Drugs.* 2008;19:819–824.
16. Petrioli R, Bargagli G, Lazzi S, et al. Thymidine phosphorylase expression in metastatic sites is predictive for response in patients with colorectal cancer treated with continuous oral capecitabine and biweekly oxaliplatin. *Anticancer Drugs.* 2010;21:313–319.
17. Naruke A, Azuma M, Takeuchi A, et al. Comparison of site-specific gene expression levels in primary tumors and synchronous lymph node metastases in advanced gastric cancer. *Gastric Cancer.* 2015;18:262–270.
18. Vallböhmer D, Kuramochi H, Shimizu D, et al. Molecular factors of 5-fluorouracil metabolism in colorectal cancer: analysis of primary tumor and lymph node metastasis. *Int J Oncol.* 2006;28:527–533.
19. Toi M, Atiqur Rahman M, Bando H, Chow LW. Thymidine phosphorylase (platelet-derived endothelial-cell growth factor) in cancer biology and treatment. *Lancet Oncol.* 2005;6:158–166.
20. Griffiths L, Dachs GU, Bicknell R, et al. The influence of oxygen tension and pH on the expression of platelet-derived endothelial cell growth factor/thymidine phosphorylase in human breast tumor cells grown in vitro and in vivo. *Cancer Res.* 1997;57:570–572.
21. Puglisi F, Andreetta C, Valent F, et al. Anthracyclines and taxanes induce the upregulation of thymidine phosphorylase in breast cancer cells. *Anticancer Drugs.* 2007;18:883–888.
22. Endo M, Shinbori N, Fukase Y, et al. Induction of thymidine phosphorylase expression and enhancement of efficacy of capecitabine or 5′-deoxy-5-fluorouridine by cyclophosphamide in mammary tumor models. *Int J Cancer.* 1999;83:127–134.
23. Zhang SH, Zhang H, He HW, et al. Lidamycin up-regulates the expression of thymidine phosphorylase and enhances the effects of capecitabine on the growth and pulmonary metastases of murine breast carcinoma. *Cancer Chemother Pharmacol.* 2013;72:777–788.

24. Takahashi M, Seki K, Nishijima K, et al. Synthesis of a radioiodinated thymidine phosphorylase inhibitor and its preliminary evaluation as a potential SPECT tracer for angiogenic enzyme expression. *J Labelled Comp Radiopharm.* 2008;51:384–387.
25. Akizawa H, Zhao S, Takahashi M, et al. In vitro and in vivo evaluations of a radioiodinated thymidine phosphorylase inhibitor as a tumor diagnostic agent for angiogenic enzyme imaging. *Nucl Med Biol.* 2010;37:427–432.
26. Li H, Zhao S, Jin Y, et al. Radiolabeled uracil derivative as a novel SPECT probe for thymidine phosphorylase: suppressed accumulation into tumor cells by target gene knockdown. *Nucl Med Commun.* 2011;32:1211–1215.
27. Zhao S, Li H, Nishijima K, et al. Relationship between biodistribution of a novel thymidine phosphorylase (TP) imaging probe and TP expression levels in normal mice. *Ann Nucl Med.* 2015;29:582–587.
28. Thanasai J, Limpaiboon T, Jearanaikoon P, et al. Effects of thymidine phosphorylase on tumor aggressiveness and 5-fluorouracil sensitivity in cholangiocarcinoma. *World J Gastroenterol.* 2010;16:1631–1638.
29. Ishikawa T, Fukase Y, Yamamoto T, et al. Antitumor activities of a novel fluoropyrimidine, N4-pentyloxycarbonyl-5′-deoxy-5-fluorocytidine (capecitabine). *Biol Pharm Bull.* 1998;21:713–717.
30. Miwa M, Ura M, Nishida M, et al. Design of a novel oral fluoropyrimidine carbamate, capecitabine, which generates 5-fluorouracil selectively in tumours by enzymes concentrated in human liver and cancer tissue. *Eur J Cancer.* 1998;34:1274–1281.
31. Yasuno H, Kurasawa M, Yanagisawa M, et al. Predictive markers of capecitabine sensitivity identified from the expression profile of pyrimidine nucleoside-metabolizing enzymes. *Oncol Rep.* 2013;29:451–458.
32. Ishikawa T, Sekiguchi F, Fukase Y, et al. Positive correlation between the efficacy of capecitabine and doxifluridine and the ratio of thymidine phosphorylase to dihydropyrimidine dehydrogenase activities in tumors in human cancer xenografts. *Cancer Res.* 1998;58:685–690.
33. Yang Q, Barbareschi M, Mori I, et al. Prognostic value of thymidine phosphorylase expression in breast carcinoma. *Int J Cancer.* 2002;97:512–517.
34. Ogawa M, Watanabe M, Mitsuyama Y, et al. Thymidine phosphorylase mRNA expression may be a predictor of response to post-operative adjuvant chemotherapy with S-1 in patients with stage III colorectal cancer. *Oncol Lett.* 2014;8:2463–2468.
35. Ishii R, Takiguchi N, Oda K, et al. Thymidine phosphorylase expression is useful in selecting adjuvant chemotherapy for stage III gastric cancer. *Int J Oncol.* 2001;19:717–722.
36. Kikuyama S, Inada T, Shimizu K, et al. p53, bcl-2 and thymidine phosphorylase as predictive markers of chemotherapy in patients with advanced and recurrent gastric cancer. *Anticancer Res.* 2001;21:2149–2153.
37. Yamamoto Y, Toi M, Tominaga T. Prediction of the effect of 5′-deoxy-5-fluorouridine by the status of angiogenic enzyme thymidine phosphorylase expression in recurrent breast cancer patients. *Oncol Rep.* 1996;3:863–865.